Low Energy Dissociation Processes of Ionized Cyclohexene: A Theoretical Insight[†,‡]

Guy Bouchoux,*,[§] Jean-Yves Salpin,[||] and Manuel Yáñez[⊥]

Laboratoire des Mécanismes Réactionnels, UMR CNRS 7651, Ecole Polytechnique, F- 91128 Palaiseau Cedex, France, Laboratoire Analyze et Environnement, UMR 8587, Institut des Sciences, Université d'Evry, boulevard F. Mitterrand, 91025 Evry Cedex, France, and Departamento de Quimica, Universidad Autonoma de Madrid, Cantoblanco, 28049 Madrid, Spain

Received: May 5, 2004; In Final Form: June 25, 2004

The major dissociation reactions of the cyclohexene radical cation, **1**, lead to the cyclopentenyl ion by methyl loss and to ionized 1,3-butadiene after elimination of C_2H_4. These two reactions are also observed during the Diels−Alder reaction between ionized butadiene and ethylene in the gas phase. The energetic and mechanistic aspects of the methyl loss process from the cyclohexene radical cation or the reaction between ionized butadiene and ethylene are discussed with the help of molecular orbital calculations at the B3LYP/6-311+G(3df,2p)//B3LYP/6-31G(d) levels. Methyl loss is demonstrated to result from successive 1,2-hydrogen shifts and ring-contraction/ring-opening steps involving, as a crucial intermediate, ionized bicyclo[1,3,0]hexane rather than the distonic ion $[CH_2CH_2CHCHCHCH_2]^{\bullet+}$ (one of the open forms of ionized cyclohexene). This latter one is however involved during the direct and retro Diels−Alder reactions. The CH_3 and C_2H_4 loss rate curves of the cyclohexene ion are calculated using the Rice−Ramsperger−Kassel−Marcus (RRKM) equation and the molecular orbital calculation results. These estimations allow understanding of the experimental observations concerning dissociations of the cyclohexene radical cation, **1**, and the collision complex formed between ionized butadiene and ethylene.

Introduction

Cation radical Diels−Alder cycloadditions, both in the condensed phase and in the gas phase, have been the subject of intense interest during the past two decades.[1−9] Surprisingly, however, the parent reaction has been explored in only a limited number of experimental[4−6] and theoretical studies.[7−10] The present status of our knowledge of the gas phase reaction between ionized 1,3-butadiene and ethylene may be summarized as follows. Starting from thermalized reactants in an ion cyclotron resonance mass spectrometer, two ionized products were identified, namely, the cyclopentenyl cation and the 1,3-butadiene radical cation resulting from a methyl loss and a methylene exchange, respectively (Scheme 1).[4] Deuterium labeling experiments reveal that the methyl loss is preceded by a quasicomplete H/D scrambling inside the transient collision complex and that the ethylene molecule eliminated during the second reaction contains specifically one methylene group from the terminal position of the 1,3-butadiene radical cation (1 or 1′) and the other from the initial neutral reactant (3 or 3′).

Identification of the cyclopentenyl ion structure has been possible from the determination of its deprotonation energy (i.e., the proton affinity of the conjugate base) experimentally, by the thermokinetic method, and theoretically, by G2MP2 molecular orbital calculations.[5] Under the very low pressure which prevails in ion cyclotron resonance (ICR) experiments, the transient collision complexes generally do not have enough time to be collisionally relaxed to their ground state before dissociation and so they are not detected. It is consequently difficult to characterize during an ICR experiment the various intermediates involved during the reactions depicted in Scheme 1. What is sure however is that all the parts of the potential energy surface explored by the system during these processes are necessarily situated below the energy level of the reactants. This thermochemical criterion, together with the results of the deuterium labeling, may be used to find reasonable pathways by means of molecular orbital calculations. This approach, suggested in our original paper,[4] has been used by Hofmann and Schaefer[8] and will be discussed later in this study. Recently, the 1,3-butadiene radical cation and ethylene reaction has been carried out under high pressure conditions in a flowing afterglow apparatus.[6] Under these conditions, adduct $[C_6H_{10}]^{\bullet+}$ ions were detected and characterized by collisions in a triple quadrupole

SCHEME 1

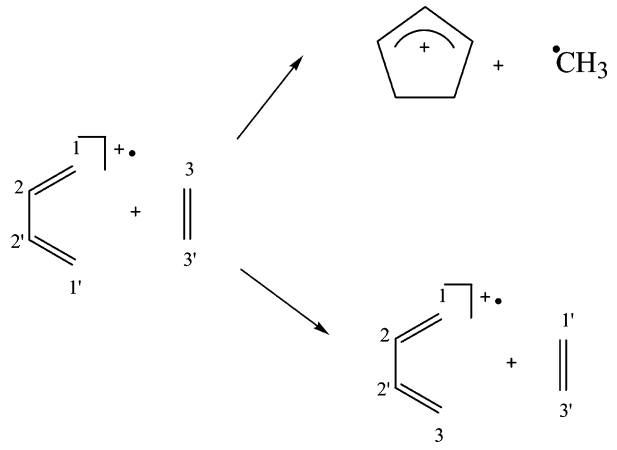

† Part of the special issue "Tomas Baer Festschrift".

‡ A paper dedicated to Prof. Tomas Baer in honor of his outstanding scientific contribution to gas-phase ion chemistry.

* Corresponding author. E-mail: bouchoux@dcmr.polytechnique.fr. Phone: (33) 1 69 33 34 00. Fax: (33) 1 69 33 30 10.

§ Ecole Polytechnique.

|| Université d'Evry.

⊥ Universidad Autonoma de Madrid.

10.1021/jp0480697 CCC: $27.50
Published on Web 08/07/2004

SCHEME 2

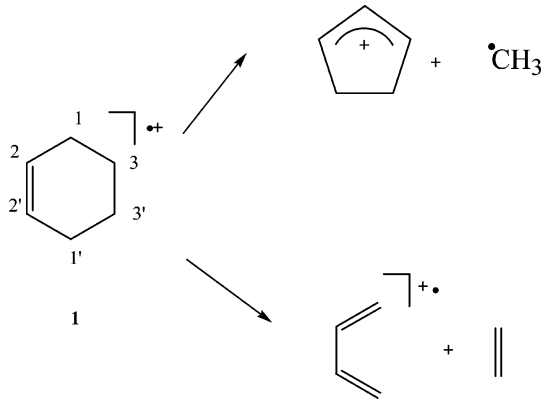

analyzer. Using the appearance curve for the formation of the $[C_5H_7]^+$ ion, and by comparison with a set of C_6H_{10} precursors (1,3-, 2,4-, and 2,4-hexadiene; 2,3-dimethyl-butadiene; 3-methyl-1,3-pentadiene; cyclohexene; 1-methyl-cyclopentene; and methylene cyclopentane), the authors proposed that the $[C_6H_{10}]^{\bullet+}$ adducts possess a 2,4-hexadiene structure.

Formally, the radical cation reaction between ethylene and the 1,3-butadiene radical cation (Scheme 1) is expected to yield the cyclohexene radical cation, **1**, according to the time-honored Diels−Alder process. The behavior of the latter radical cation has been studied for a long time.[11−19] Its major dissociation route, as well as many other $[C_6H_{10}]^{\bullet+}$ ions,[14,15] leads to the $[C_5H_7]^+$ ion (Scheme 2).

It is noteworthy that the methyl loss is the lowest energy pathway and that the AE$[C_5H_7]^+$ values, from cyclohexene, measured by Winters and Collins,[17] by Traeger and Lossing,[19] and by Li and Baer[20] are within ∼0.1 eV and point to the formation of the cyclopentenyl ion at its thermochemical threshold. Moreover, the exclusive formation of the cylopentenyl structure has also been established from deprotonation energy determination.[5] Deuterium labeling shows that this fragmentation is preceded by a complete H/D exchange when low internal energy precursors are sampled;[11−14] by contrast, a preferred elimination of a methyl containing a methylene in position 1(1′) (Scheme 2) is noted at short observation times (i.e., at energies high enough to attain a dissociation rate of $\sim 10^{11}$ s^{-1}).[11−13]

The second dissociation pathway of the cyclohexene radical cation, **1**, is the so-called retro Diels−Alder fragmentation which regenerates the 1,3-butadiene radical cation and ethylene (Scheme 2). Again, appearance energy determinations point to the formation of the dissociation products close to their thermochemical threshold.[17,20] Information provided by the deuterium labeling indicates a preference for the elimination of C_2H_4 containing the hydrogen atoms in positions 3 and 3′ at high internal energy, and a statistical distribution of the labels at low internal energy. This latter phenomenon has been suggested to originate from 1,3-allylic-hydrogen shifts on the intact cyclohexene ring.[11−13] Direct and reverse cation radical Diels−Alder reactions have been investigated using ab initio molecular orbital calculations by Bauld,[7] Hofmann and Schaefer,[8,9] and Haberl et al.[10] The authors conclude that stepwise processes connecting ionized cyclohexene, **1**, with the 1,3-butadiene radical cation plus ethylene occur via an open chain distonic intermediate situated ∼140 kJ/mol above ionized cyclohexene.

Despite this valuable experimental and theoretical information, several important questions remain unanswered. In particular, what is the mechanism of the methyl elimination from ionized cyclohexene, **1**? Further, is this mechanism applicable to the methyl elimination observed in the reaction between the 1,3-butadiene radical cation and ethylene? Finally, what is the involvement of ionized cyclohexene, **1**, and ionized 2,4-hexadiene during the radical cation Diels−Alder process?

The goal of the present study is thus to bring new theoretical results answering these fundamental questions. As shown below, a new and complete interpretation of the lowest energy routes followed by ionized cyclohexene, **1**, and the reactants of the parent Diels−Alder reaction will be proposed. It is based on a large investigation of the potential energy profile connecting the various species considered by means of density functional theory (DFT) molecular orbital calculations at the B3LYP/6-311+G(3df,2p)//B3LYP/6-31G(d) level. Our results emphasize the key role of bicyclo[3,1,0]hexane, methyl-1- and methyl-3-cyclopentene, and their 1,3-diyl(distonic) isomers during the isomerization processes. A rationalization of the available data will be discussed in the light of these results and statistical rate constant calculations.

Computational Section

The potential energy profile associated with the direct and reverse Diels−Alder processes and with the methyl loss reaction leading to the cyclopentenyl cation has been examined using the DFT method at the B3LYP/6-31G(d) level. Zero point vibrational energies were estimated at this level, and more accurate energies have been obtained from single point calculations at the B3LYP/6-311+G(3df,2p) level. All calculations have been undertaken using the Gaussian98 suite of programs.[21]

In general, geometries obtained using the aforementioned DFT method are in fairly good agreement with experimental values,[22−29] and the unscaled harmonic vibrational frequencies are closer to experiment than those obtained by using other correlated methods such as MP2.[30,31] Furthermore, different comparisons between B3LYP and different ab initio correlated procedures[8−10,32−36] show the reliability of this DFT approach when combined with flexible enough basis set expansions.

The conical intersection associated with the evolution of some of the radicals along the reaction mechanisms under study were located at the CASSCF(5,6)/6-31G* level, which is the level of theory used for systems of similar size and characteristics in the literature.[37]

Microcanonical rate constant calculations were performed in the framework of the Rice−Ramsperger−Kassel−Marcus (RRKM)[40] and statistical phase space[41] theories using the TSTPST package elaborated by Chesnavich et al.[42] The sum and density of states are calculated using the Beyer−Swinehart algorithm with vibrational degrees of freedom, including hindered rotations, treated as harmonic oscillators.

Results and Discussion

The Thermochemical Frame. Since thermochemistry dictates the feasibility of the observed reaction processes, a brief summary of the presently available data is given as a preamble. Heats of formation obtained at 298 and 0 K for the cyclohexene radical cation, **1**, and its dissociation products are presented in Table 1.

The appearance energies of the $[C_5H_7]^+$ and $[C_4H_6]^{\bullet+}$ fragment ions originating from cyclohexene were determined in the 1970s from electron ionization experiments.[17−19] As mentioned in the Introduction, methyl loss is the lowest energy pathway of the two competitive channels. Winters and Collins[17] utilized the energy distribution difference method of determination of appearance energies after calibration of the energy scale with krypton and xenon. They obtained AE$[C_5H_7]^+$ and AE$[C_4H_6]^{\bullet+}$ values of 10.18 and 10.67 eV, respectively, and

TABLE 1: Relevant Thermochemical Data (kJ/mol)

species	$\Delta_f H^\circ_{298}$	relative ΔH°_{298}	$\Delta_f H^\circ_0$	relative ΔH°_0
[cyclohexene]$^{\bullet+}$	859.2 ± 1.4[a]	0	890.5[b]	0
[cyclopentenyl]$^+$	840.6 ± 4.1[c]		860.8[b]	
$^\bullet CH_3$	145.8[d]		149.0[d]	
[cyclopentenyl]$^+$ + $^\bullet CH_3$	986.3	127.1	1009.8	119.3
[1,3-butadiene]$^{\bullet+}$	984.1 ± 1.1[e]		998.61[b]	
C_2H_4	52.2[d]		60.7[d]	
[1,3-butadiene]$^{\bullet+}$ + C_2H_4	1036.6	177.4	1059.3	168.8

[a] From IE(cyclohexene) = 8.95 ± 0.01 eV and $\Delta_f H^\circ_{298}$(cyclohexene) = −4.3 ± 1.0 kJ/mol (ref 38). [b] Calculated using $H^\circ_{298} - H^\circ_0$ corrections estimated at the B3LYP/6-31G(d) level and 1.05 and 8.47 kJ/mol for the elements C(graphite) and H_2(g), respectively (ref 38). [c] From ref 5. [d] From ref 23. [e] From IE(1,3-butadiene) = 9.072 ± 0.007 eV and $\Delta_f H^\circ_{298}$(1,3-butadiene) = 108.8 ± 0.8 kJ/mol (ref 38).

an ionization energy of IE(cyclohexene) = 8.92 eV, in excellent agreement with the 8.95 eV value obtained by photoelectron of photoionization experiments.[2,38,39] Using a monoenergetic electron beam device, Traeger and Lossing[19] obtained AE-$[C_5H_7]^+$ = 10.27 eV, in correct agreement with Winters and Collins.[17] By contrast, Praet,[18] who used the extrapolated voltage difference method, reported AE energies higher by ∼1.0 eV than the values reported by the preceding authors. The reason for this discrepancy lies probably in a wrong calibration of the energy scale, since the cyclohexene ionization energy is itself overestimated by ∼0.6 eV in Praet's report.[18] More recently, Li and Baer[20] explored the behavior of cyclohexene by threshold photoelectron−photoion coincidence spectroscopy; they obtained AE values for both $[C_5H_7]^+$ and $[C_4H_6]^{\bullet+}$ within ∼0.1 eV of the results reported by Winters and Collins[17] and Traeger and Lossing.[19]

It is essential to note that the differences between the appearance and ionization energies for methyl loss and ethylene loss, 119[17]−127[19] and 166[17] kJ/mol, respectively, are close to the enthalpy difference between the dissociation products and the cyclohexene molecule (Table 1). It is thus clear that formation of the cyclopentyl cation and ionized 1,3-butadiene occurs at the corresponding thermochemical thresholds.

A corollary observation is that all the reaction intermediates and transition structures separating **1** from its dissociation products should lie below a 298 K enthalpy of ∼990 kJ/mol for the methyl loss and ∼1040 kJ/mol for the retro Diels−Alder reaction. This leaves open the route for isomerization into a lot of stable structures, such as ionized allenes, dienes, cyclopentane derivatives, or cyclobutane derivatives, as attested by the tabulation of their heats of formation.[38,39] What seems to be excluded however is the passage through acetylenic structures before the methyl loss.

The Lowest Energy Route for the Methyl Loss from the Cyclohexene Radical Cation, 1. In 1999, Hofmann and Schaefer[8] investigated pathways for the methyl loss from the adduct formed during the Diels−Alder reaction between the 1,3-butadiene radical cation and ethylene. The pathway of lowest energy identified by the authors at the UCCSD(T)/DZP//UMP2/DZP+ZPE level of theory is summarized in Scheme 3.

During this process, ethylene adds to the 1,3-butadiene radical cation to form the distonic intermediate **2** which undergoes a 1,5-hydrogen migration leading to the 1,4-hexadiene radical cation, **3**. Intramolecular cyclization produces various forms of the 1,3-diyl(distonic) methyl cyclopentane intermediate, **4**, in which a 1,2-hydrogen shift gives rise to the 3-methyl cyclopentene radical cation, **5**, the obvious precursor of the dissociation products, the cyclopentenyl cation plus CH_3. Formation of the cyclohexene radical cation, **1**, from the distonic ion **2** has been shown to need practically no critical energy by the same authors.[9]

It is clear that the reaction sequence presented in Scheme 3 does not provide a correct basis for the interpretation of the behavior of ionized cyclohexene, **1**, since the appearance energy determinations point to the formation of the cyclopentenyl cation plus CH_3 at their thermochemical threshold. In fact, according

SCHEME 3

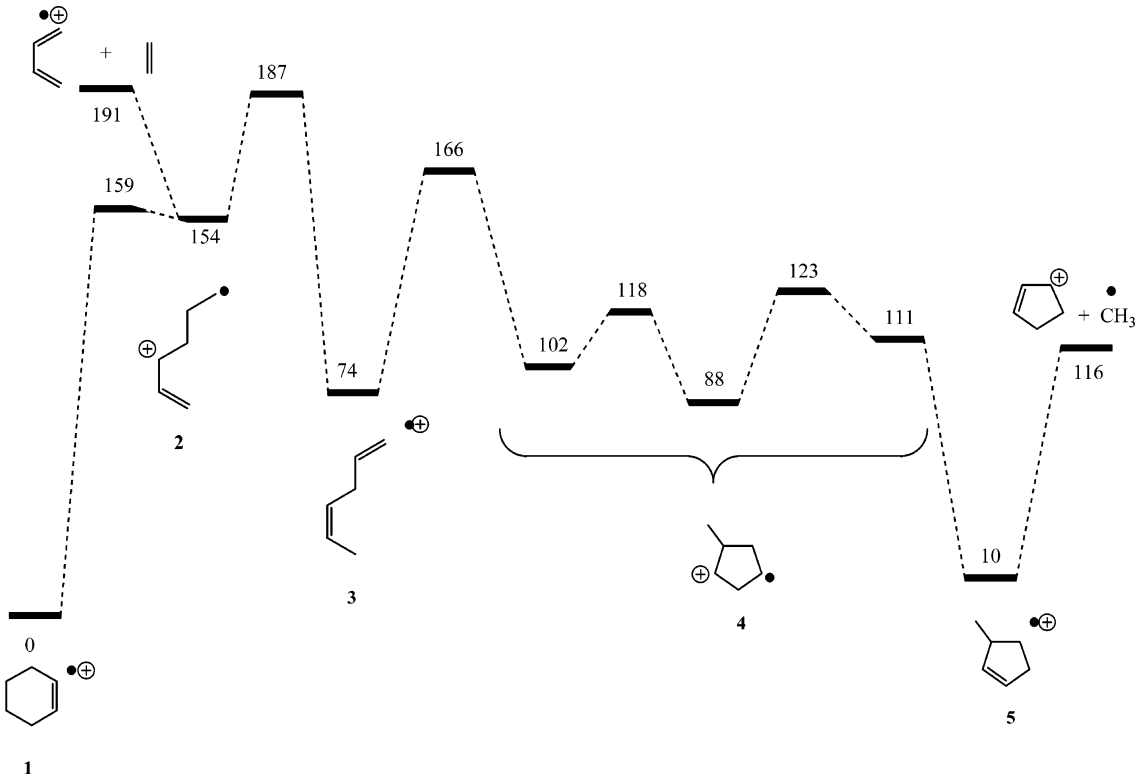

TABLE 2: Total Energies (*E*, hartrees), Zero Point Energies (ZPE, hartrees), and Relative 0 K Energies (Δ*E*, kJ/mol) of the $[C_6H_{10}]^{\bullet+}$ Structures Investigated

$[C_6H_{10}]^{\bullet+}$ species	E^a	ZPE[b]	Δ*E*
1	−234.408 695	0.143 570	0
7	−234.380 150	0.140 795	67
6(planar)	−234.378 971	0.140 961	71
6(chair)	−234.383 588	0.144 020	67
8	−234.393 378	0.144 210	42
9	−234.348 211	0.143 382	158
5	−234.404 034	0.142 041	8
14	−234.421 868	0.141 105	−41
15	−234.401 535	0.142 195	15
13	−234.381 160	0.143 242	71
11	−234.360 186	0.140 480	119
16	−234.339 710	0.142 557	178
12	−234.385 176	0.137 614	46
10	−234.375 028	0.141 834	84
$C_5H_7^+$	−194.451 352	0.104 608	
$CH_3^\bullet$	−39.857 742 9	0.029 833	
$C_5H_7^+ + CH_3$	−234.359 095	0.134 441	106
$C_4H_6^{\bullet+}$	−155.730 256	0.084 927	
C_2H_4	−78.621 085	0.051 228	
$C_4H_6^{\bullet+} + C_2H_4$	−234.351 341	0.136 155	131
1/7	−234.378 622	0.140 489	71
6/7	−234.364 372	0.139 909	106
6/6	−234.378 55	0.141 491	74
7/8	−234.365 678	0.140 975	106
8/9	−234.336 546	0.142 535	187
9/15	−234.347 578	0.142 942	159
13/14	−234.361 678	0.139 287	111
13/16	−234.331 460	0.141 870	198
11/13	−234.351 504	0.139 036	138
11/12	−234.338 336	0.138 459	171
5/11	−234.352 164	0.140 715	141
14/12	−234.378 560	0.138 686	66
5/12	−234.382 834	0.138 659	55
8/13	−234.381 073	0.142 889	72
ts610	−234.370 366	0.141 808	96
ts16	−234.353 493	0.140 825	138

[a] B3LYP/6-311+G(3df,2p)//B3LYP/6-31G(d) level. [b] B3LYP/6-31G(d) level (without scaling).

SCHEME 4

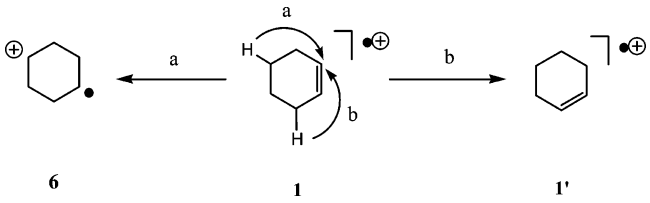

6 **1** **1'**

to UCCSD(T)/DZP//UMP2/DZP+ZPE calculations, the dissociation products are situated 116 kJ/mol (experimental, 119 kJ/mol; see Table 1) above **1**, and consequently, even the first step of the above process, that is, the ring opening **1** → **2**, should be excluded because of its too large energy requirement! We thus investigate other reaction paths such as hydrogen migrations and ring contractions with the objective to find processes which need less energy than the upper limit of ∼120 kJ/mol.

The corresponding total and relative energies obtained during the present study at the B3LYP/6-311+G(3df,2p)//B3LYP/6-31G(d)+ZPE level are gathered in Table 2, and key structures are given in the Supporting Information.

The first considered elementary steps, starting from ionized cyclohexene, **1**, are presented in Schemes 4 and 5.

The degenerate 1,3-hydrogen shift **1** → **1′** (Scheme 4) has been studied by Hofmann and Schaefer[8] who found a critical energy of ∼170 kJ/mol, clearly a value that is too high to retain this reaction. Similarly, the external 1,3-hydrogen shift **1** → **6** leading to the 1,4-diyl(distonic) cyclohexane radical cation, **6**, is associated with a too large critical energy (138 kJ/mol).

SCHEME 5

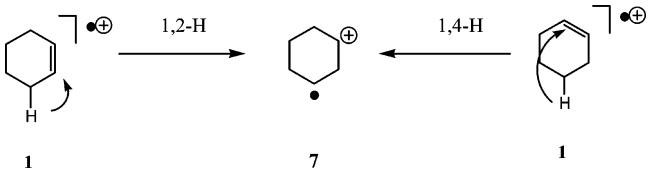

1 **7** **1**

SCHEME 6

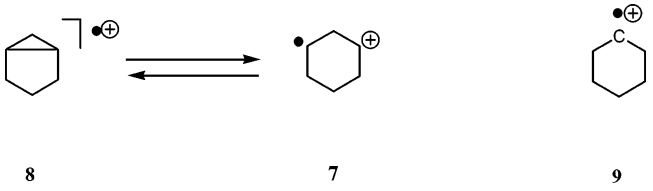

8 **7** **9**

By contrast, the formation of the 1,3-diyl(distonic) cyclohexane radical cation, **7**, via a 1,2-hydrogen shift from **1** appears to be possible (Scheme 5). At the B3LYP/6-311+G(3df,2p)//B3LYP/6-31G(d)+ZPE level, this reaction, **1** → **7**, passes through a transition structure situated 71 kJ/mol above **1** and leads to the 1,3-diyl cyclohexane radical cation, **7**, a structure which appears to be only weakly stabilized (4 kJ/mol) with respect to the transition structure **1**/**7**. Another pathway for the formation of ion **7** is the 1,4-hydrogen migration, **1** → **7**, indicated in Scheme 5. This reaction however needs a constrained folding of the cyclohexene skeleton which results in a critical energy as high as 185 kJ/mol, clearly a value that is too large to be considered here.

If the direct generation of the 1,4-diyl(distonic) cyclohexane radical cation, **6**, from **1** may reasonably be excluded, its formation from **7** appears to be feasible. Accordingly, the isomerization **7** → **6** by a 1,2-hydrogen shift passes by a transition structure with a relative energy of 106 kJ/mol. The 1,4-diyl(distonic) cyclohexane radical cation, **6,** is then produced in a quasiplanar conformation situated 71 kJ/mol above **1** and isomerizes easily to its more stable chair conformer (relative energy, 67 kJ/mol). These two conformers are connected by a quite low energy barrier, **6**(planar) → **6**(chair), of 2 kJ/mol.

Two other structures keeping the cyclohexane ring arrangement have been finally considered: bicyclo[3,1,0]hexane, **8**, and cyclohexyl carbene, **9** (Scheme 6).

B3LYP/6-311+G(3df,2p)//B3LYP/6-31G(d)+ZPE calculation places radical cations **8** and **9** 42 and 158 kJ/mol, respectively, above **1**. Thus, the latter carbenoid ion should not be retained as a possible reaction intermediate, while **8** constitutes obviously a favorable candidate. Furthermore, calculation shows that the ring closure **7** → **8** may occur slightly below the upper thermochemical limit, since the transition structure **7**/**8** possesses a relative energy equal to 106 kJ/mol. A similar ring closure of the 1,4-diyl ion **6** to give ionized bicyclo[2,2,0]hexane has been excluded because experimental thermochemistry indicates that the latter ion is 135 kJ/mol above ionized cyclohexane, **1**.[38,39]

At this stage, it appears that the most easily accessible structure from **1**, en route to the methyl loss, is the 1,3-diyl cyclohexane radical cation, **7**, which in turn may isomerize to **8** or **6**. It is worth mentioning that the region of the potential energy surface in the surroundings of structure **7** is centered around a conical intersection,[37] which at the CASSCF(5,6)/6-31G* level of theory lies 44 kJ/mol above structure **7**. From this conical intersection, one of the reaction coordinates will

SCHEME 7

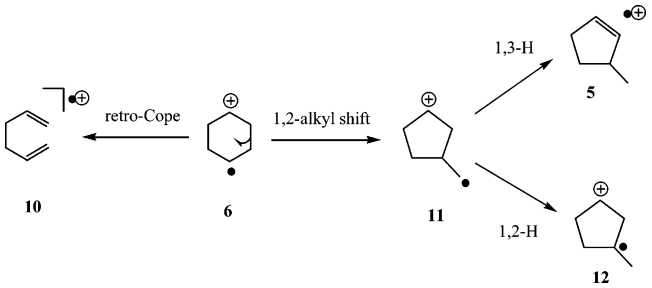

SCHEME 8

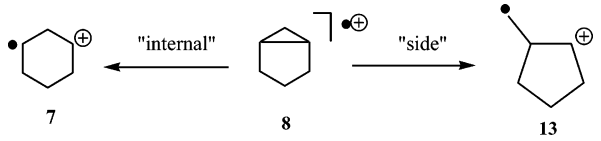

correspond to the C(1)−C(3) stretching displacement leading to bicyclo[3,1,0]hexane, **8**, and the other, to a rocking of the methylene groups at positions C4 and C5 that would favor the 1,4-hydrogen shift that would connect **7** and **1**.

The possible evolutions of the distonic ion **6** should involve the breaking of one of the C(2)C(3) bonds, as presented in Scheme 7.

The simple ring opening of ion **6** (the retro Cope reaction) leads to ionized 1,5-hexadiene, **10**. However, the experimental heat of formation of **10** is 122 kJ/mol higher than that of ionized cyclohexene[39] and, therefore, this reaction is probably unlikely to occur before methyl loss. This hypothesis is not entirely corroborated by the calculations. Accordingly, at the B3LYP/6-311+G(3df,2p)/B3LYP/6-31G(d) level, the relative energy of **10** is only 84 kJ/mol and that of the transition structure **6**/**10** is equal to 96 kJ/mol. The second possible evolution of **6** consists of a C(2)C(3) bond breaking coupled with a C(2)C(4) bond forming. This 1,2-alkyl shift generates the 3-methylene cyclopentyl distonic ion, **11**, whose calculated relative energy (119 kJ/mol) is close to the upper thermochemical limit. Isomerization of **11** by a 1,3- or 1,2-hydrogen shift in order to produce either ionized 3-methyl cyclopentene, **5**, or ionized 1,3-diyl methyl cyclopentane, **12** (Scheme 7), is a high energy process. The energies of the corresponding transition structures **5**/**11** and **11**/**12** are calculated to be 141 and 171 kJ/mol, respectively; this clearly excludes the participation of **11** in the searched reaction pathway.

The reaction potentialities of the bicyclo[3,1,0]hexane structure, **8**, remain to be explored. The behavior of such a species, bearing an ionized cyclopropane ring, is expected to rely on the weakness of this structural moiety. The "internal" cyclopropane ring opening, **8** → **7**, which has been discussed above enters into this category. The other possibility is the "side" cyclopropane ring opening which would give rise to the 2-methylene cyclopentyl distonic ion, **13** (Scheme 8).

This latter reaction is the most favored one; its transition structure (relative energy, 72 kJ/mol) is very close in structure and in energy to the distonic ion **13** (relative energy, 71 kJ/mol).

The remaining part of the travel consists, starting from **13**, of successive hydrogen migrations on the methyl cyclopentane skeleton that produce ionized 3-methyl cyclopentene, **5**, the most likely precursor of the $[C_5H_7]^+$ cyclopentenyl fragment ion. The lowest energy route, presented in Scheme 9, involves exclusively 1,2-hydrogen shifts.

SCHEME 9

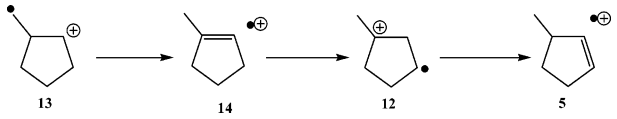

SCHEME 10

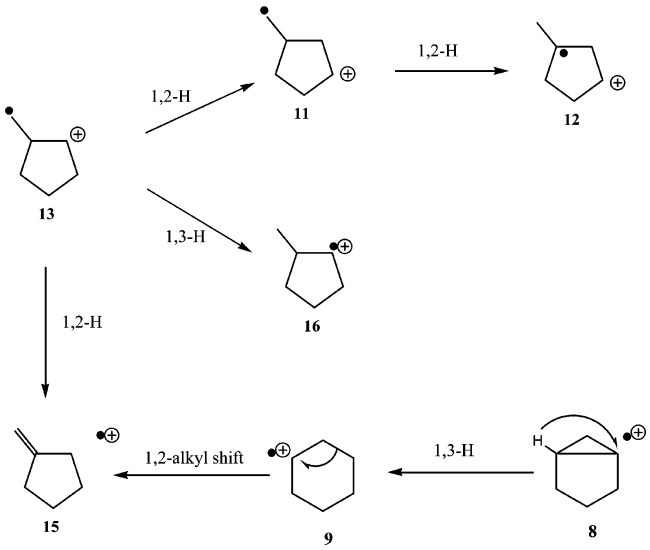

The highest transition structure corresponds to the step **13** → **14**; its relative energy (111 kJ/mol) is very close to the energy level of the dissociation products (calculated, 106 kJ/mol; experimental, 123 kJ/mol). Structures **14** and **5** are the most stable species bearing a cyclopentane skeleton; their relative energies are −41 and 8 kJ/mol, respectively. Interconversion of **5** and **14** via the distonic intermediate **12** is a facile process; the top of the overall energy barrier (corresponding to the step **14** → **12**) is 40 kJ/mol below the dissociation products.

Other reactions were explored in the vicinity of structures **12** and **13** (Scheme 10), for example, isomerization of the 2-methylene cyclopentyl cation, **13**, by 1,2- and 1,3-hydrogen shifts leading to the 3-methylene cyclopentyl ion, **11**, and the carbenic ion **16**; formation of the 3-methylene cyclopentyl ion, **11**, by a 1,2-hydrogen shift from **12**; or involvement of ionized methylene cyclopentane, **16**, by cyclization of cyclohexyl carbene, **9**, formed by a 1,3-hydrogen migration inside the precursor **8**. All these possibilities should be excluded on the basis of their too energetic transition structures or even, in some cases, of the too high relative energy of the stable species itself (e.g., **9** and **16**) (see Table 2). One should note that reaction **13** → **15** is associated with a very low critical energy, and thus, the latter structure may be easily produced. However, it constitutes a cul-de-sac in the present part of the potential energy surface, since its isomerization into ionized 3-methyl cyclopentene, **5**, needs 180 kJ/mol of critical energy.[8]

In summary, the lowest energy route for methyl loss from ionized cyclohexene, **1**, involves a combination of 1,2-hydrogen shifts and the crucial ring-closure/ring-opening event, **7** → **8** → **13**. A general view of the corresponding part of the calculated 0 K energy surface is presented in Scheme 11. It is important to note that the 0 K calculated endothermicity of the reaction **1** → the cyclopentenyl cation plus CH_3, **17** (106 kJ/mol), matches closely the ΔH_0° value deduced from the experimental ΔH_{298}° value (119 kJ/mol, Table 1). Furthermore, the isomerization of **1** into **14** appears to involve transition structures close in energy to the products **17**, a situation which strongly determines the

SCHEME 11

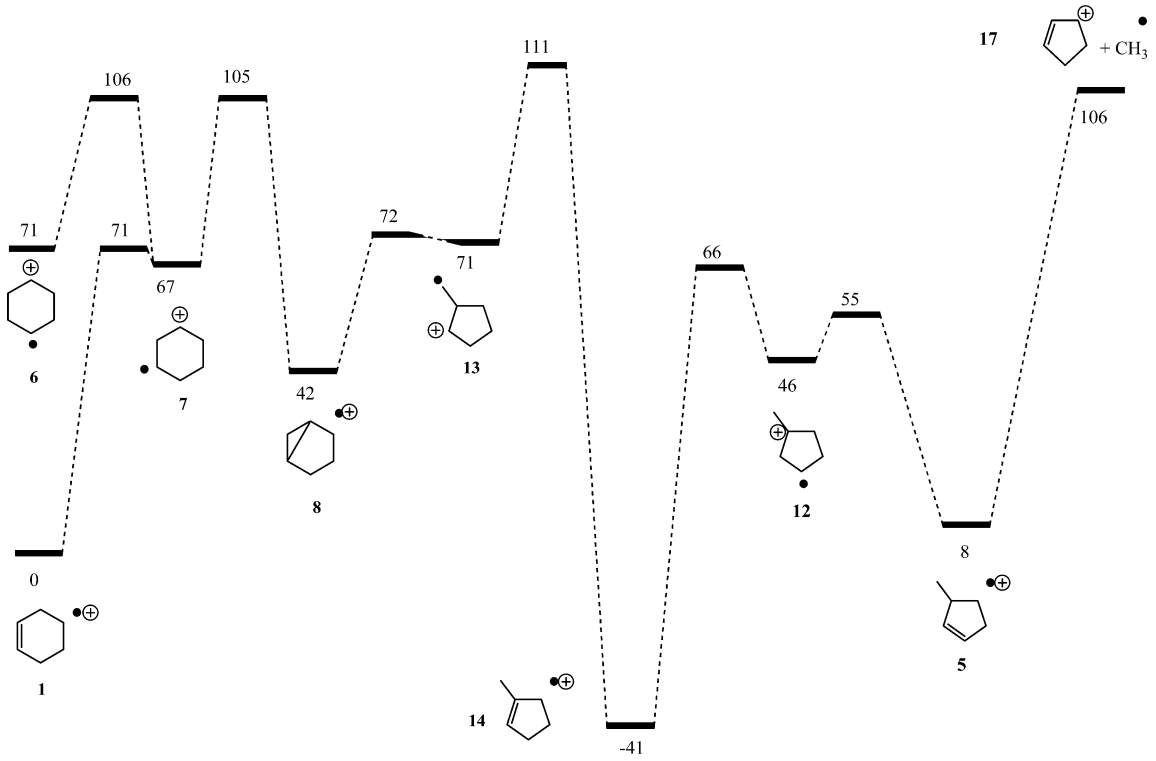

kinetic behavior of **1** as depicted in the dissociation rate modeling section.

The Lowest Energy Route for the Ethylene Loss from the Cyclohexene Radical Cation, 1. The second dissociation reaction of ionized cyclohexene, **1**, is the retro Diels−Alder process. As mentioned in the Introduction, this reaction has been extensively studied experimentally[11−16] and theoretically.[7,9,10] Thus, only the salient results will be indicated here. The most recent molecular orbital studies point to a potential energy surface connecting **1** and ionized 1,3-butadiene plus ethylene, **18**, via the distonic ion $[CH_2CH_2CHCHCHCH_2]^{\bullet+}$, **2**. According to CCSD(T)/DZP[9] or QCISD(T)/6-31G*[10] calculations including ZPVE, the latter structure is situated 36[9]−32[10] kJ/mol below **1** and the transition structure **1**/**2** is situated only 15[9]−5[10] kJ/mol above **2**. Considering the relative ΔH_0° value of **1** and **18** quoted in Table 1 (169 kJ/mol) and the above-mentioned molecular orbital data, the relevant part of the 0 K energy surface may be constructed (see Scheme 12). Since the participation of ionized vinyl cyclobutane, **19**, to the chemistry of **1** has been suggested,[4,9,10] we present in Scheme 12 its calculated energy level (118 kJ/mol)[9] and that of the transition structure **2**/**19** which lies ∼10 kJ/mol above **2**.[9]

Kinetics of Cyclohexene Radical Cation Dissociations. To examine the competition between the methyl and ethylene losses from **1**, unimolecular dissociation rates of both processes have been calculated using the RRKM theory.[40] Considering the large number of steps of the studied reactions, a simplified approach of this system has been adopted.

Roughly, the potential energy profile along the CH_3 loss coordinate is characterized by the deep valley created by the 1-methyl cyclopentene radical cation, **14**, and by a large **1** → **14** isomerization barrier which presents the peculiarity to be close in energy to the dissociation products **17**. We thus consider a simplified kinetic model where the reversible isomerization step **1** ↔ **14** precedes the dissociation **14** → **17**. Each individual rate coefficient, $k_{1\rightarrow14}$, $k_{14\rightarrow1}$, and $k_{14\rightarrow17}$, has been calculated using the B3LYP/6-31G(d) frequencies and rotational constants

SCHEME 12

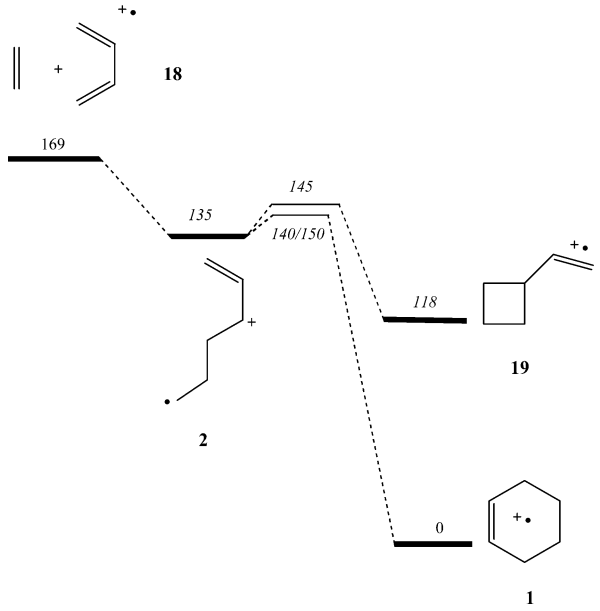

summarized in Table 3. For the isomerization step **1** ↔ **14**, the transition structure considered is that of the energy determining 1,2-hydrogen shift, **13**/**14**. Concerning the dissociation **14** → **17**, we used the orbiting transition state model,[41] which makes use of the vibrational frequencies of the separated species, to estimate the corresponding rate constant. Critical energies were based on the experimental 0 K energy differences between **1** and **14** and **17**, that is, −0.39[39] and 1.23 eV (Table 1), respectively. Two values of the critical energy for the forward reaction **1** → **14** (Scheme 13) were considered; the first one, E° = 1.23 eV, comes from the evidence provided by the molecular orbital calculations that the transition structure **13**/**14** is close in energy to the products **17**. Incidence of the lowering of this isomerization barrier **1** ↔ **14** has been explored

TABLE 3: Summary of the Calculated (B3LYP/6-31G*) Parameters Used in the RRKM Statistical Rate Constant Calculations

	[cyclohexene]$^{\bullet+}$, **1**
rotational constants (GHz):	4.70, 4.51, 2.53
frequencies (cm^{-1}):	154, 200, 273, 447, 486, 607, 661, 720, 824, 827, 865, 875, 910, 1005, 1033, 1066, 1071, 1086, 1172, 1203, 1260, 1268, 1353, 1360, 1365, 1384, 1392, 1419, 1476, 1521, 1523, 1557, 2869, 2878, 3023, 3028, 3062, 3072, 3134, 3134, 3198, 3250
	TS **13**/**14**
rotational constants (GHz):	6.77, 3.12, 2.28
frequencies (cm^{-1}):	166, 214, 337, 445, 489, 573, 620, 728, 787, 839, 877, 890, 896, 919, 929, 1002, 1037, 1078, 1160, 1203, 1243, 1275, 1289, 1325, 1336, 1376, 1433, 1449, 1492, 1515, 1531, 2469, 2958, 3080, 3087, 3093, 3145, 3160, 3177, 3218, 3294
	[3-methyl cyclopentene]$^{\bullet+}$, **14**
rotational constants (GHz):	6.90, 3.03, 3.23
frequencies (cm^{-1}):	89, 109, 183, 333, 407, 594, 616, 700, 774, 836, 877, 914, 940, 947, 973, 1025, 1053, 1127, 1178, 1201, 1248, 1290, 1318, 1343, 1380, 1390, 1398, 1420, 1463, 1494, 1520, 1547, 2935, 2962, 2996, 3030, 3056, 3092, 3096, 3156, 3159, 3224
	[cyclopentenyl]$^{+}$
rotational constants (GHz):	8.05, 7.60, 4.10
frequencies (cm^{-1}):	200, 386, 592, 786, 813, 835, 882, 935, 935, 1023, 1037, 1047, 1133, 1136, 1164, 1204, 1312, 1320, 1373, 1422, 1431, 1509, 1534, 3032, 3035, 3053, 3056, 3228, 3231, 3269
	$CH_3^{\bullet}$
rotational constants (GHz):	285.0, 285.0, 142.6
frequencies (cm^{-1}):	448, 1430, 1430, 3144, 3319, 3319
	TS **1**/**2**
rotational constants (GHz):	6.21, 2.04, 1.74
frequencies (cm^{-1}):	77, 163, 238, 293, 325, 367, 505, 539, 563, 792, 870, 891, 921, 1004, 1028, 1039, 1047, 1094, 1144, 1196, 1238, 1249, 1268, 1297, 1329, 1462, 1491, 1495, 1543, 1554, 1612, 3114, 3131, 3175, 3179, 3187, 3190, 3200, 3209, 3282, 3282
	[1,3-butadiene]$^{\bullet+}$
rotational constants (GHz):	41.0, 4.4, 4.0
frequencies (cm^{-1}):	188, 295, 438, 517, 526, 917, 943, 1016, 1022, 1046, 1051, 1284, 1297, 1302, 1376, 1518, 1544, 1658, 3180, 3180, 3199, 3208, 3285, 3285
	C_2H_4
rotational constants (GHz):	147.0, 30.0, 25.0
frequencies (cm^{-1}):	835, 966, 966, 1070, 1248, 1396, 1494, 1720, 3152, 3167, 3222, 3248

SCHEME 13: Methyl Loss

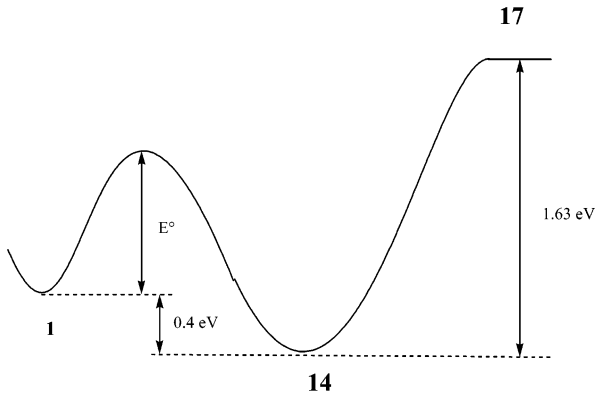

by using a critical energy, $E°$, arbitrarily equal to 1.13 eV. To estimate the overall dissociation rate for the process **1** → **17**, $k(CH_3)$, it may be assumed that the steady state approximation is applicable to the vibrationally excited intermediate **14**. Under these conditions, $k(CH_3)$ may be expressed as

$$k(CH_3) = k_{1\rightarrow 14}k_{14\rightarrow 17}/[k_{1\rightarrow 14} + k_{14\rightarrow 1} + k_{14\rightarrow 17}]$$

Evolutions of the individual rate coefficients $k_{1\rightarrow 14}$, $k_{14\rightarrow 1}$, and $k_{14\rightarrow 17}$ and of $k(CH_3)$ as a function of the internal energy, E, of the dissociating species **1** are displayed in Figure 1.

It appears clearly from examination of Figure 1 that the inequality $k_{1\rightarrow 14} > k_{14\rightarrow 1}$ always holds. Similarly, $k_{14\rightarrow 17}$ is significantly higher than $k_{1\rightarrow 14}$ because of the looseness of the transition state for the separation of the products, **14** → **17**, with respect to the isomerization step **1** → **14**. As a consequence,

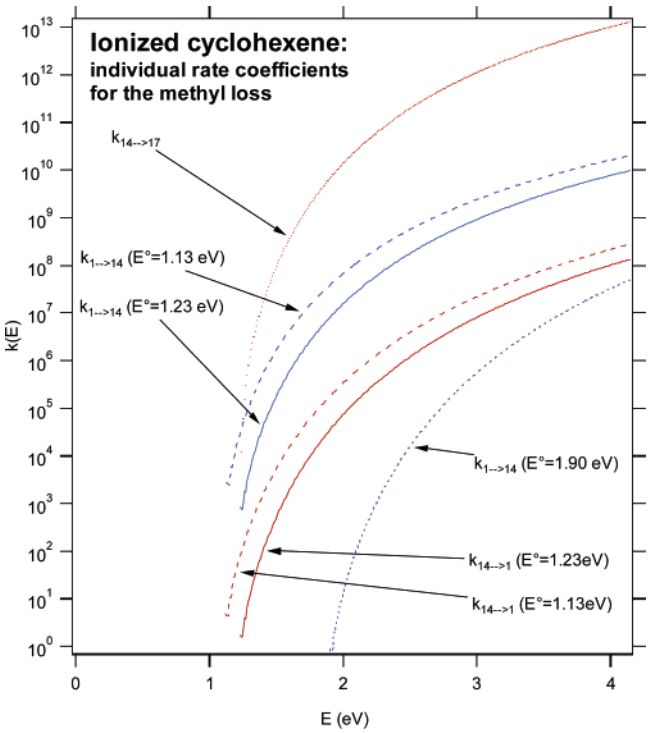

Figure 1. Calculated RRKM rate coefficients for the methyl loss route: **1** ↔ **14** → **17**.

the overall reaction rate $k(CH_3)$ is practically equal to $k_{1\rightarrow 14}$, that is, to the rate coefficient of the slowest process. The two $k(CH_3)$ curves calculated for $E° = 1.23$ and 1.13 eV are reported

SCHEME 14: Ethylene Loss

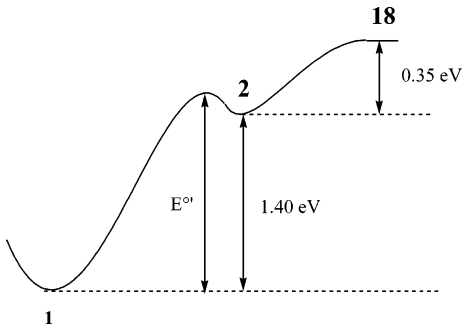

in Figure 3. It must be emphasized that $E^\circ = 1.23$ eV constitutes the upper bound for the critical energy of the isomerization barrier en route to the methyl loss; thus, the corresponding $k(CH_3)$ curve is the lowest limit for the methyl elimination rate. At this stage, it is of interest to consider the methyl loss process suggested to occur during the radical cation Diels−Alder reaction summarized in Scheme 3. According to Hofmann and Shaefer,[8] the rate determining step of the reaction is the 1,5-hydrogen migration **2** → **3**, the transition structure of which being situated 187 kJ/mol above **1**. If we roughly consider the model of Scheme 13 with $E^\circ = 1.90$ eV, the resulting reaction rate $k(CH_3)$ (Figure 3) appears to be 10^{-5}−10^{-2} lower than the limiting $k(CH_3)$ curve calculated with $E^\circ = 1.23$ eV in the explored energy range.

Concerning the retro Diels−Alder reaction, our kinetic modeling used the **1** ↔ **2** → **18** sequence and the simplified potential energy profile sketched in Scheme 14. The 0 K relative energies used in the calculations are based on the experimental enthalpy difference between **1** and **18** (1.75 eV, Table 1) and on the molecular orbital calculations of refs 9 and 10; thus, two values of 1.45 and 1.55 eV have been considered for the critical energy $E^{\circ\prime}$. As illustrated in Figure 2, for both $E^{\circ\prime}$ values, the rate constant for separation of the products $k_{2\rightarrow 18}$ is found to be larger than $k_{2\rightarrow 1}$ and $k_{1\rightarrow 2}$. Consequently, the overall rate constant for the retro Diels−Alder (RDA) reaction, given, in the assumption of the steady state approximation on intermediate ion **2**, by the expression

$$k(\mathrm{RDA}) = k_{1\rightarrow 2}k_{2\rightarrow 18}/[k_{1\rightarrow 2} + k_{2\rightarrow 18} + k_{2\rightarrow 1}]$$

may be equated to $k_{1\rightarrow 2}$. The two relevant k(RDA) curves obtained with $E^{\circ\prime} = 1.45$ and 1.55 eV are presented in Figure 3 and compared with the $k(CH_3)$ results.

The results of this kinetic modeling should be now compared with the experimental information. It has been observed from field ionization kinetic experiments[11−13] that the retro Diels−Alder reaction dominates for cyclohexene radical ions, **1**, at high internal energy, while at low internal energy the predominant process is the elimination of the methyl radical. Moreover, the average rate constants for the two dissociation reactions were shown to be equal at a time close to 10^{-9} s. In agreement with these observations, the major unimolecular dissociation of metastable cyclohexene radical ions, **1**, in the field free region of a magnetic tandem mass spectrometer, is the methyl loss.[14,15] Finally, when the 1,3-butadiene radical cation and ethylene are allowed to react at thermal energies in a Fourier transform mass spectrometer, a branching ratio of 1.5 favoring methyl loss has been observed.[4] Under these experimental conditions, the sampled species correspond to cyclohexene radical ions, **1**, containing ∼2.0 eV of internal energy.

All these findings are clearly verified here by the evolution of k(RDA) and $k(CH_3)$ presented in Figure 3 with $E^\circ = 1.23$ eV and $E^{\circ\prime} = 1.45$ eV. It is remarkable that the crossing of the k(RDA) and $k(CH_3)$ curves occurs for rate constant values of $\sim 10^9$ s^{-1}, that is, for observation times of $\sim 10^{-9}$ s, thus corroborating the field ionization kinetic results. The close evolution of both rate constants confirms that the CH_3 loss is preceded by a rate determining step of a transition state energy close to that of the dissociation products **17**. From this point of view, it seems unlikely that a reaction preceded by a 1,5-hydrogen migration with a critical energy of 1.90 eV should compete, at either internal energy, E, with the CH_3 loss process described here (Figure 3). Finally, we note that the overall rate coefficients shown in Figure 3 present starting values close to 10^5 s^{-1} and are consequently at the origin of a limited kinetic shift during appearance energy determination.

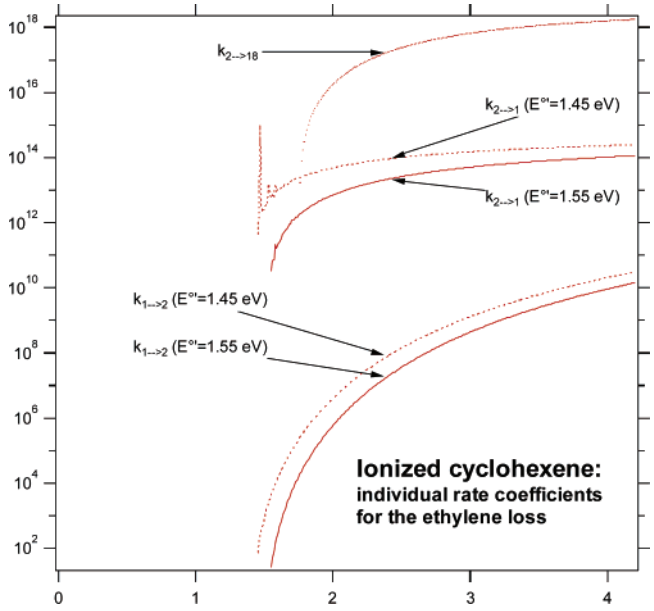

Figure 2. Calculated RRKM rate coefficients for the ethylene loss route (the retro Diels−Alder reaction): **1** ↔ **2** → **18**.

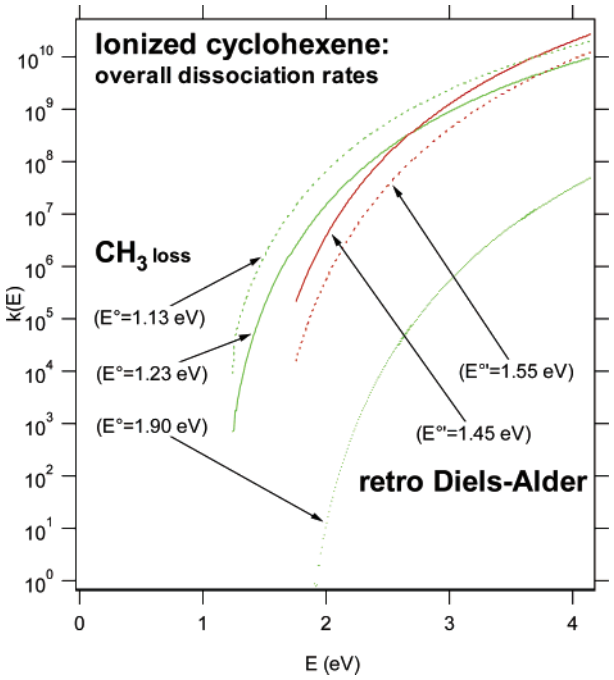

Figure 3. Overall dissociation rates calculated for the methyl loss and the retro Diels−Alder reactions.

H/D Exchanges in Labeled Species. Deuterium labeling experiments show that eliminations of both CH_3 and C_2H_4 from cyclohexene radical ions, **1**, of low internal energy are accompanied by complete H/D scrambling.[11−15] According to the present molecular orbital calculations, the mechanism responsible of this phenomenon is the reversible 1,2-hydrogen shift **1** ↔ **7**, not the degenerate 1,3-hydrogen migration **1** ↔ **1** originally suggested[11] which may be clearly excluded on energetic grounds. It is of interest to note that a complete H/D scrambling has been also observed for the methyl elimination during the reaction between the 1,3-butadiene radical cation and ethylene,[4] thus suggesting passage through **1** before the CH_3 elimination. By contrast, the selectivity observed during the same experiments for the C_2H_4 loss is obviously originating from competition with another process bypassing ionized cyclohexene, **1**. From a mechanistic point of view, a [2 + 1] cycloaddition/cycloreversion reaction involving ionized vinylcyclobutane, **19**, offers a simple explanation for the fact that the eliminated C_2H_4 contains a methylene group from the terminal position of both reactants.[4] Results of molecular orbital calculation[9,10] (Scheme 12) suggest that, after its formation from the reactants **18**, the distonic ion **2** isomerizes equivalently (and easily) to **1** or **19** but that the back reaction occurs more readily from **19** than from **1**, since the critical energies differ by 118 kJ/mol.

Conclusion

The present B3LYP/6-311+G(3df,2p)//B3LYP/6-31G(d) molecular orbital calculations combined with RRKM statistical reaction rate estimations shed new light on ionized cyclohexene chemistry. First, the energetic and mechanistic aspects of the methyl loss process from the cyclohexene radical cation, **1**, or the reaction between ionized butadiene and ethylene have been established. Methyl loss is demonstrated to result from successive 1,2-hydrogen shifts and ring-contraction/ring-opening steps involving, as a crucial intermediate, ionized bicyclo[1,3,0]-hexane. This reaction mechanism is presently the process of lowest energy identified. It is the lone mechanism that is compatible with the appearance energy determinations. It is also probably the best candidate for the explanation of the methyl loss observed during the cation radical Diels−Alder reaction.

Second, the kinetic modeling of the retro Diels−Alder reaction from **1** shows that the first step, the formation of the distonic ion $[CH_2CH_2CHCHCHCH_2]^{\bullet+}$, is crucial in lowering the *k*(RDA) rate constant values to a level comparable to that of the methyl loss, *k*(CH_3). This competition, attested by various experimental results (branching ratio, H/D exchanges, appearance energy determination) concerning the cyclohexene radical cation, **1**, or the reaction between ionized butadiene and ethylene, is satisfactorily reproduced by the present theoretical findings.

Acknowledgment. The authors thank Professor Tomas Baer for the communication of his PEPICO results on cyclohexene and 3-methyl cyclopentene and Professor Olaf Wiest for the vibrationnal frequencies of the transition structure **1**/**2**. This research has been partially supported by the DGI Project No. BQU2003-00894.

Supporting Information Available: Cartesian coordinates of the optimized geometries (B3LYP/6-31G(d) level) of the various minima and transition states listed in Table 2. This material is available free of charge via the Internet at http://pubs.acs.org.

References and Notes

(1) For a review on radical cation cycloadditions in the condensed phase, see: Bauld, N. L. *Tetrahedron* **1989**, *45*, 5307−5363.

(2) For examples of the application of radical cation cycloadditions to organic synthesis, see the literature cited in refs 7−9 and the following more recent studies: (a) Peglow, T.; Blechert, S.; Steckhan, E. *Chem.−Eur. J.* **1998**, *4*, 107−112. (b) Peglow, T.; Blechert, S.; Steckhan, E. *Chem. Commun.* **1999**, *4*, 433−434. (c) Rössler, U.; Blechert, S.; Steckhan, E. *Tetrahedron Lett.* **1999**, *4*, 7075−7078. (d) Saettel, N. J.; Oxgaard, J.; Wiest, O. *Eur. J. Org. Chem.* **2001**, 1429−1439. (e) Saettel, N. J.; Wiest, O.; Singleton, D. A.; Meyer, M. P. *J. Am. Chem. Soc.* **2002**, *124*, 11552−11559.

(3) For a review on radical cation cycloadditions in the gas phase, see: Dass, C. *Mass Spectrom. Rev.* **1990**, *9*, 1−36.

(4) Bouchoux, G.; Salpin, J.-Y. *Rapid. Commun. Mass Spectrom.* **1994**, *8*, 325−328.

(5) Bouchoux, G.; Salpin, J.-Y. *Chem. Phys. Lett.* **2002**, *366*, 510−519.

(6) Hu, H.; Wenthold, P. G. *J. Phys. Chem. A* **2002**, *106*, 10550−10553.

(7) Bauld, N. L. *J. Am. Chem. Soc.* **1992**, *114*, 5800−5804.

(8) Hofmann, M.; Schaefer, H. F. I. *J. Phys. Chem. A* **1999**, *103*, 8895−8905.

(9) Hofmann, M.; Schaefer, H. F. I. *J. Am. Chem. Soc.* **1999**, *121*, 6719−6729.

(10) Haberl, U.; Wiest, O.; Steckhan, E. *J. Am. Chem. Soc.* **1999**, *121*, 6730−6736.

(11) Derrick, P. J.; Falick, A. M.; Burlingame, A. L. *J. Am. Chem. Soc.* **1972**, *94*, 6794−6802.

(12) Burinsky, D. J.; Glish, G. L.; Cooks, R. G.; Zwinselman, J. J.; Nibbering, N. M. M. *J. Am. Chem. Soc.* **1981**, *103*, 465−467.

(13) Nibbering, N. M. M. *Mass Spectrom. Rev.* **1984**, *3*, 445−477.

(14) Wolkoff, P.; Holmes, J. L. *Can. J. Chem.* **1979**, *57*, 348−354.

(15) Wolkoff, P.; Holmes, J. L. *Can. J. Chem.* **1980**, *58*, 251−257.

(16) Hu, H.; Wenthold, P. G. *J. Am. Soc. Mass Spectrom.* **2001**, *12*, 840−845.

(17) Winters, R. E.; Collins, J. H. *Org. Mass Spectrom.* **1969**, *2*, 299−308.

(18) Praet, M. T. *Org. Mass Spectrom.* **1970**, *4*, 65−80.

(19) Lossing, F. P.; Traeger, J. C. *Int. J. Mass Spectrom. Ion Phys.* **1976**, *19*, 9−22.

(20) Baer, T. Personal communication, 2003.

(21) Frisch, M. J.; Trucks, G. W.; Schlegel, H. B.; Scuseria, G. E.; Robb, M. A.; Cheeseman, J. R.; Zakrzewski, V. G.; Montgomery, J. A.; Stratmann, R. E., Jr.; Burant, J. C.; Dapprich, S.; Millam, J. M.; Daniels, A. D.; Kudin, K. N.; Strain, M. C.; Farkas, O.; Tomasi, J.; Barone, V.; Cossi, M.; Cammi, R.; Mennucci, B.; Pomelli, C.; Adamo, C.; Clifford, S.; Ochterski, J.; Petersson, G. A.; Ayala, P. Y.; Morokuma, Q.; Cui, K.; Malick, D. K.; Rabuck, A. D.; Raghavachari, K.; Foresman, J. B.; Cioslowski, J.; Ortiz, J. V.; Stefanov, B. B.; Liu, G.; Liashenko, A.; Piskorz, P.; Komaromi, I.; Gomperts, R.; Martin, R. L.; Fox, D. J.; Keith, T.; Al-Laham, M. A.; Peng, C. Y.; Nanayakkara, A.; Gonzalez, C.; Challacombe, M.; Gill, P. M. W.; Johnson, B.; Chen, W.; Wong, M. W.; Andres, J. L.; Gonzalez, C.; Head-Gordon, M.; Replogle, E. S.; Pople, J. A. *Gaussian 98*, revision A.6; Gaussian, Inc.: Pittsburgh, PA, 1998.

(22) Sim, F.; St-Amant, A.; Papai, I.; Salahub, D. R. *J. Am. Chem. Soc.* **1992**, *114*, 4391.

(23) Kim, K.; Jordan, K. D. *J. Phys. Chem.* **1994**, *98*, 10089−10094.

(24) Bauschlicher, C. W. *Chem. Phys. Lett.* **1995**, *246*, 40−44.

(25) Llamas-Saiz, A. L.; Foces-Foces, C.; Mo, O.; Yanez, M.; Elguero, E.; Elguero, J. *J. Comput. Chem.* **1995**, *16*, 263−272.

(26) Bauschlicher, J. C. W.; Partridge, H. *J. Chem. Phys.* **1995**, *103*, 1788−1791.

(27) Mebel, A. M.; Morokuma, K.; Lin, M. C. *J. Chem. Phys.* **1995**, *103*, 7414−7421.

(28) Montgomery, J. A., Jr.; Frisch, M. J.; Ochterski, J. W.; Peterson, G. A. *J. Chem. Phys.* **1999**, *110*, 2822−2827.

(29) Curtiss, L. A.; Redfern, P. C.; Raghavachari, K.; Pople, J. A. *J. Chem. Phys.* **2001**, *114*, 108−117.

(30) Stephens, P. J.; Devlin, F. J.; Chabalowski, C. F.; Frisch, M. J. *J. Phys. Chem.* **1994**, *98*, 11623−11627.

(31) Wong, M. W. *Chem. Phys. Lett.* **1996**, *256*, 391−399.

(32) Smith, B. J.; Radom, L. *Chem. Phys. Lett.* **1994**, *231*, 345−351.

(33) Gonzalez, L.; Mo, O.; Yanez, M. *J. Comput. Chem.* **1997**, *18*, 1124−1135.

(34) Gonzalez, L.; Mo, O.; Yanez, M. *J. Chem. Phys.* **1998**, *109*, 139−150.

(35) Petersson, G. A.; Malick, D. K.; Wilson, W. G.; W., O. J.; Montgomery, J. A., Jr.; Frisch, M. J. *J. Chem. Phys.* **1998**, *109*, 10570−10579.
(36) Curtiss, L. A.; Raghavachari, K.; Redfern, P. C.; Pople, J. A. *J. Chem. Phys.* **2000**, *112*, 7374−7383.
(37) Blancafort, L.; Adam, W.; González, D.; Olivucci, M.; Vreven, T.; Robb, M. A. *J. Am. Chem. Soc.* **1999**, *121*, 10583−10590.
(38) NIST webbook. http://webbook.nist.gov/chemistry.
(39) Lias, S. G.; Bartmess, J. E.; Liebman, J. F.; Holmes, J. L.; Levin, R. D.; Mallard, W. G. Gas-Phase Ion and Neutral Thermochemistry. *J. Phys. Chem. Ref. Data* **1988**, *17* (Suppl. 1).
(40) Baer, T.; Hase, W. L. *Unimolecular Reaction Dynamics: Theory and Experiments*; Oxford University Press: New York, 1996.
(41) Chesnavich, W. J.; Bowers, M. T. *J. Chem. Phys.* **1977**, *66*, 2306.
(42) Chesnavich, W. J.; Bass, L.; Grice, M. E.; Song, K.; Webb, D. A. *Program QCPE 557*.